Journal of the Physical Society of Japan
Vol. 69, No. 10, October, 2000, pp. 3228-3232

Collision Strength Measurement for Electron-Impact Excitation of Neonlike Barium

Nobuyuki NAKAMURA[1,*], Daiji KATO[1], Nozomu MIURA[2] and Shunsuke OHTANI[1,2]

[1] *Cold Trapped Ions Project, ICORP, JST, Chofu, Tokyo 182-0024*
[2] *The University of Electro-Communications, Chofu, Tokyo 182-8585*

(Received February 23, 2000)

Relative collision strengths have been measured for electron-impact excitation to $(2p_{1/2}^{-1}3s)_{J=1}$ and $(2p_{3/2}^{-1}3d_{5/2})_{J=1}$ in neonlike barium, whose wave functions are strongly mixed with each other. An experimental method has been developed for the collision strength measurement from X-ray observations by using the Tokyo electron beam ion trap. X-ray transitions from these excited states were observed with a flat crystal spectrometer. The electron energy was adjusted to 5.02 keV which is just above the threshold, and the electron energy width was narrowed to 16 ± 8 eV by reducing the electron beam current. This allowed us to exclude indirect excitation followed by radiative cascades. The experimental collision strength ratio was found to be larger than the distorted-wave calculation by [Zhang and Sampson: At. Data Nucl. Data Tables **43** (1989) 1]. This discrepancy is probably attributed to the contribution of resonant excitation.

KEYWORDS: X-ray spectroscopy, neonlike ions, highly charged ions, electron beam ion trap, electron-impact excitation

§1. Introduction

Since neonlike ions have a closed shell structure, their abundance in hot plasmas is high for a wide range of plasma parameters. As a result, neonlike ions can be widely used for many kinds of application, such as X-ray lasers and plasma diagnostics.[1)] For these applications, systematic studies of transition wavelengths, oscillator strengths and collision strengths in neonlike ions are strongly needed.

In our previous study,[2)] wavelengths for several $n = 3$ to 2 transitions in the neonlike ions with $Z = 53$–56 were measured. Through these measurements, strong configuration mixing between $(2p_{1/2}^{-1}3s)_{J=1}$ and $(2p_{3/2}^{-1}3d_{5/2})_{J=1}$ at the atomic number $Z \sim 55$ was found. In this Z region, it is inadequate to represent each of these states as a single electron configuration. In the following text, we then refer to the state having the largest mixing coefficient for $(2p_{3/2}^{-1}3d_{5/2})_{J=1}$ as $|3D\rangle$, and that having the largest coefficient for $(2p_{1/2}^{-1}3s)_{J=1}$ as $|3F\rangle$, following the notations used by Loulergue and Nussbaumer.[3)] This strong configuration mixing results in anomalous behavior in Z-dependence of the oscillator strengths. For example, theoretical calculations by Kagawa *et al.*[4)] showed that the oscillator strength for the $2p^6 \rightarrow |3F\rangle$ transition is enhanced while that for the $2p^6 \rightarrow |3D\rangle$ transition is suppressed at $Z \sim 55$. Recently, Ivanova and Grant[5)] also investigated Z-dependence of the oscillator strengths, and argued that study of atomic structure in neonlike ions is very important for X-ray laser modeling.

On the other hand, collision strengths for electron-impact excitation of neonlike ions are also affected by the strong configuration mixing. Zhang and Sampson[6)] systematically calculated the collision strengths for electron-impact excitation to $n = 3$ and 4 excited levels in neonlike ions using the relativistic distorted-wave method. Their calculation showed that the collision strengths for $|3F\rangle$ and $|3D\rangle$ have Z-dependence similar to that of the oscillator strengths, i.e. the collision strength for the $2p^6 \rightarrow |3F\rangle$ excitation is enhanced while that for the $2p^6 \rightarrow |3D\rangle$ excitation is suppressed at $Z \sim 55$.

From an experimental point of view, it is very hard to measure electron-impact-excitation cross sections for highly charged ions because of extremely low target density. An electron beam ion trap[7)] is the only apparatus which enable ones to study electron collisions with very highly charged ions in the interaction energy range of $\sim$ 1 to $\sim$ 200 keV.[8)] Marrs *et al.*[7)] measured the electron-impact-excitation cross sections for $|3D\rangle$ and $(2p_{1/2}^{-1}3d_{3/2})_{J=1}$ in neonlike barium. They also measured the excitation cross sections as a function of electron beam energy for $|3D\rangle$ and $(2p_{3/2}^{-1}3s)_{J=2}$ in neonlike barium[9)] and $n = 2$ excited levels in heliumlike titanium.[10)] These measurements generally involve indirect excitation processes, such as excitation followed by radiative cascades, and hence may be undesirable to investigate the effect of strong configuration mixing. To exclude completely indirect excitation processes, measurements should be made by using an electron beam with just above the threshold energy.

In this paper, we present measurements of relative collision strength for the electron-impact excitation to $|3D\rangle$ and $|3F\rangle$ in neonlike barium, Ba^{46+}. Marrs *et al.*[11)] also measured the intensity ratio between $|3D\rangle \rightarrow 2p^6$

* E-mail: nakamura@hci.jst.go.jp

(spectral line denoted $3D$) and $|3F\rangle \to 2p^6$ (spectral line denoted $3F$). Their measurements seem to be a preliminary work. Although the details of their experimental condition are not clear, the electron beam obtained on the usual operational condition was probably used because their interest was to study the contribution of indirect excitation processes. Thus the energy spread of the electron beam in their measurements is considered to be 50 eV FWHM or more.[7,10] With such an energy spread, indirect excitation processes cannot be eliminated even if the electron energy is just above the threshold because the nearest upper level is very close to the levels of interest. Meanwhile the present measurement was done at electron energy of 5.024 keV, which is about 40 eV below the nearest upper level, with a energy spread of 16 eV. The narrow spread made it possible to exclude completely the cascading effects.

§2. Experiments

In the present study, an EBIT was used to observe X-ray transitions in neonlike barium. There are several processes by which $n = 3$ excited levels of neonlike barium are produced by electron impact in the trap region of an EBIT:

(i) direct excitation (DE)

$$2s^2 2p^6 + e^- \to 2l^{-1}3l' + e^-, \tag{2.1}$$

(ii) resonant excitation (RE)

$$2s^2 2p^6 + e^- \to 2l^{-1}n'l'n''l'' \to 2l^{-1}3l''' + e^-, \tag{2.2}$$

(iii) excitation followed by radiative cascades (RC)

$$2s^2 2p^6 + e^- \to 2l^{-1}n'l' + e^- \to 2l^{-1}3l'' + h\nu + e^-. \tag{2.3}$$

Since not only neonlike barium but also sodiumlike and fluorinelike barium generally exist in an EBIT, the following processes should also be considered:

(iv) inner shell ionization of sodiumlike barium (II)

$$2s^2 2p^6 3l + e^- \to 2l^{-1}3l' + 2e^-, \tag{2.4}$$

(v) radiative recombination to fluorinelike barium (RR)

$$2s^2 2p^5 + e^- \to 2s^2 2p^5 nl + h\nu \to 2s^2 2p^5 3l' + h\nu + h\nu'. \tag{2.5}$$

Figure 1 shows $n = 3$ excited levels near $|3D\rangle$ and $|3F\rangle$ in neonlike barium. As shown in the figure, several levels which are forbidden to decay directly to the ground state can decay to $|3F\rangle$ via electric dipole transitions. Consequently, the electron energy should be in between the level energies of $|3F\rangle$ and that of $(2p^{-1}_{1/2}3p_{1/2})_{J=1}$ (represented as p^*p^* in Fig. 1) to completely exclude RC processes. The present measurement was thus done at the electron energy of 5.024 keV. At this energy, the processes II and RR are also excluded because the energy is well below both the threshold for inner shell ionization of sodiumlike barium and the ionization energy of neonlike barium. Consequently, only DE and RE can contribute to excitation to $|3D\rangle$ and $|3F\rangle$ in the present experiment.

Neonlike barium was produced and trapped in the Tokyo EBIT, which is described in detail elsewhere.[12-14] Barium was evaporated from the cathode of the electron gun and ionized in the trap region. X-ray transitions excited by an electron beam was observed with a flat crystal spectrometer.[2] Since the radiation source in an electron beam ion trap is a line source whose width is about 60 μm, it is possible to use wavelength dispersive spectrometers without an entrance slit. The spectrometer used in this study consisted of a flat LiF(200) crystal with an area of $100 \times 50\,\mathrm{mm}^2$ and a position sensitive proportional counter (PSPC) with a backgammon-type cathode.[15] The crystal was placed at 730 mm away from the center of the trap and the PSPC at 740 mm away from the crystal. The effective volume of the PSPC was $100 \times 30 \times 4\,\mathrm{mm}^3$ in which PR gas (90% Ar+10% CH_4) was filled at a pressure of 4 atm. Typical resolution in position for the present PSPC was about 300 μm. The spectrometer was operated in vacuo ($\sim 10^{-7}$ torr) to avoid absorption by air. A beryllium foil with a thickness of 50 μm was used to separate the vacuum of the EBIT ($\sim 10^{-9}$ torr) from that of the spectrometer.

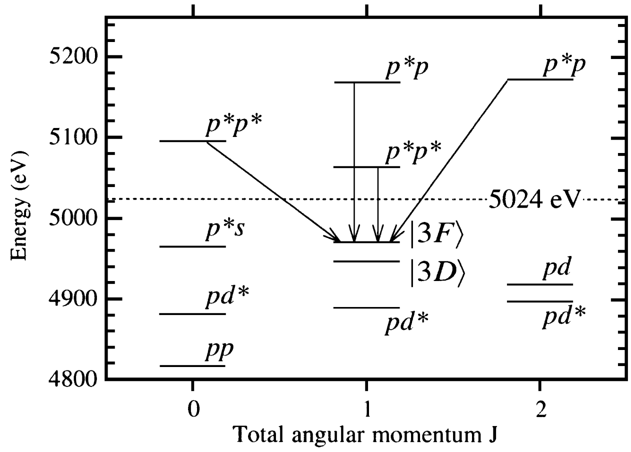

Fig. 1. Energy levels of neonlike barium near $|3D\rangle$ and $|3F\rangle$. For the levels other than $|3D\rangle$ and $|3F\rangle$, the first letter represents the orbital angular momentum of the $n = 2$ hole, and the second letter that of the excited electron. Asterisks represent the total angular momentum of the hole or the electron; l if $j = l + \frac{1}{2}$ and l^* if $j = l - \frac{1}{2}$. Thus, for example, "p^*p" represents $(2p^{-1}_{1/2}3p_{3/2})$. The electric dipole transitions are shown by arrows. A dotted line represents the electron energy at which the present measurement was done.

In the present observation, X-ray line intensity is an important quantity; therefore, the detection efficiency of the PSPC should be constant independent of the detection position. Uniformity of the detection efficiency was examined by illuminating the PSPC with an X-ray tube. Since the source size of the tube was about 300 μm and the distance between the tube and the PSPC was about 1 m, the illumination on the PSPC was sufficiently uniform. Thus, the uniformity was found to be better than $\pm 3\%$ for the region of interest.

The electron beam energy was measured by observing radiative recombination processes for bare and hydrogenlike argon with a solid state detector. Figure 2(a) shows an X-ray spectrum for the radiative recombination to the $n = 1$ levels in bare and hydrogenlike argon. To observe this spectrum, an argon and neon gas mixture was introduced from one of the observation ports. Neon was

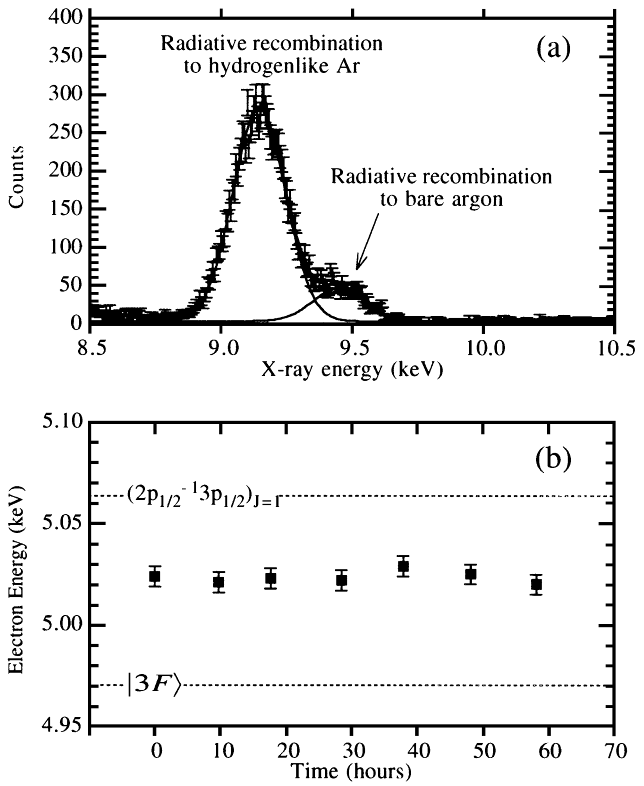

Fig. 2. (a) X-ray spectrum for radiative recombination to $n = 1$ in hydrogenlike and bare argon taken with a solid state detector. Solid lines represent the Gaussian line profiles fitted to the observed spectrum. (b) Stability of the electron energy throughout the observation period. Dotted lines represent the level energies of $|3F\rangle$ and $(2p_{1/2}^{-1}3p_{1/2})_{J=1}$.

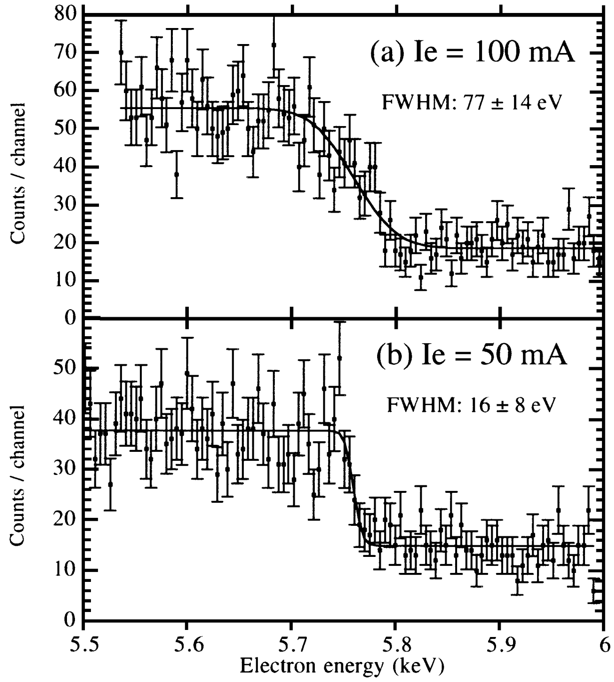

Fig. 3. Electron energy dependence of the radiative recombination X-ray intensity for hydrogenlike argon observed through a Ta foil 7.5 μm thick; (a) for the electron beam current of 100 mA, (b) 50 mA. Solid lines represent the error function fitted to the data. Error bars represent the statistical error.

introduced as coolant[16] which was needed to produce and trap bare and hydrogenlike argon efficiently. The X-ray energy scale was calibrated using two radioisotopes, ^{55}Fe and ^{57}Co.[17] The X-ray energies of the radiative recombination peaks were determined by fitting Gaussian profiles to the data. In the fitting procedure, it was assumed that the energy difference between the two peaks is 305.34 eV[18] and their widths were the same. Thus the X-ray energy was determined to be 9.144 keV for the radiative recombination peak of hydrogenlike argon. By subtracting the ionization energy of heliumlike argon[18] from this value 9.144 keV, the electron energy was determined to be 5.024 ± 0.005 keV. The uncertainty was estimated from the uncertainty in the X-ray energy scale and the statistical error. As will be described later, it took about 60 hours to obtain one X-ray spectrum with the crystal spectrometer. For this reason, the electron energy measurements were made once per about 10 hours to examine the stability. Figure 2(b) shows the time dependence of the electron energy. As shown in the figure, the electron energy was stable within the uncertainty during 60 hours of observation time.

The electron energy spread was separately measured by the method used by Levine *et al.*[19] The radiative recombination X-ray line of hydrogenlike argon was observed through a Ta foil 7.5 μm thick with scanning the electron energy so that the radiative recombination X-ray energy crossed the L-absorption edge of Ta (9.88 keV). Figure 3 shows the electron energy dependence of the radiative recombination X-ray intensity for the electron current of (a) 100 mA and (b) 50 mA. By fitting error functions to the data, the electron energy spreads were determined to be 77 ± 14 eV and 16 ± 8 eV (FWHM), respectively. It is known that the electron energy spread decreases as the beam current decreases.[20] The energy spread of 77 eV is so wide that electrons in the high energy tail of the distribution can excite the $(2p_{1/2}^{-1}3p_{1/2})_{J=1}$ level (labeled p^*p^* in Fig. 1). Consequently, the collision strength measurement was performed at the electron current of 50 mA. The electron energy in the energy spread measurement is slightly different from that in the collision strength measurement. However, we consider that the electron energy spread is the same for both experimental conditions because all operational parameters are the same except for the voltage applied to the drift tube assembly.

§3. Results and Discussion

Figure 4(a) shows a typical X-ray spectrum obtained with the beam energy of 5.024 keV. The $3D$ and the $3F$ line are observed at the X-ray energy of about 4938 eV and 4960 eV, respectively. These lines were identified in the previous observation.[2] Although most of the other peaks have not been identified yet, they are considered to be lines from barium ions whose charge state is 45+ or less. The relatively low electron energy and the current made the abundance and the total amount of neonlike barium small. Consequently, the X-ray radiation was so weak that it took about 60 hours to obtain the spectrum

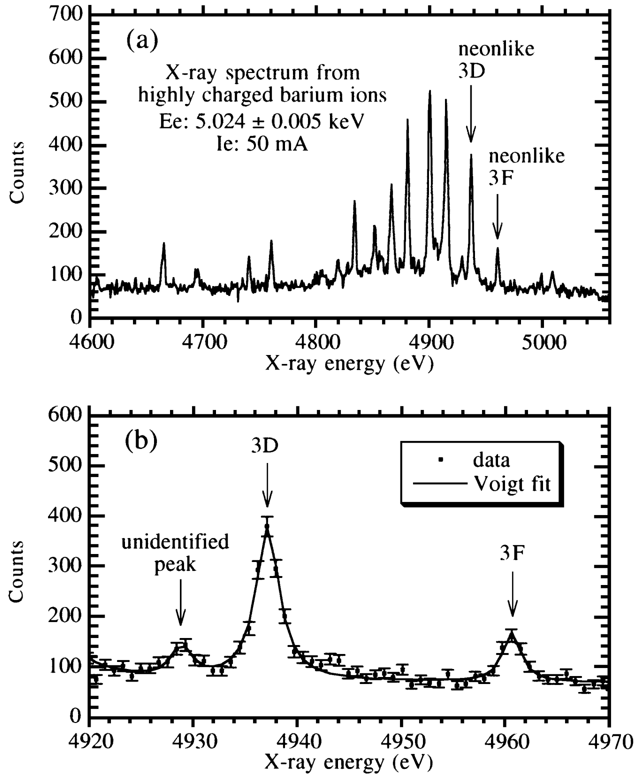

Fig. 4. (a) High resolution X-ray spectrum from highly charged barium ions observed with a flat crystal spectrometer. Ee and Ie are the energy and the current of the electron beam, respectively. (b) Expanded spectrum for the region near $3D$ and $3F$. A solid line represents the fitted spectrum.

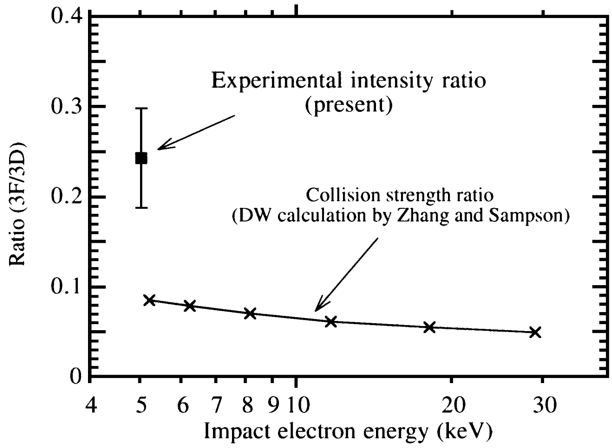

Fig. 5. Experimental intensity ratio between $3F$ and $3D$ (solid square). Crosses represent the collision strength ratio obtained from relativistic distorted wave calculations by Zhang and Sampson.[6)]

shown in Fig. 4.

The radiation excited by a directional electron beam is generally not isotropic.[21)] Furthermore, the reflectivity of a crystal strongly depends on the direction of the polarization.[22)] Thus in order to obtain the reliable collision strengths from the present observation, the magnetic sublevel distribution in the excitation process and the consequent polarization of the emitted X-rays should be known. Zhang and Sampson[23)] calculated the collision strengths Ω_0 and Ω_1 for electron-impact excitation to the magnetic sublevels $M_J = 0$ and 1 in neonlike iron (Z=26) and molybdenum (42). The results showed that, for both elements and for the whole impact energy range studied, the value Ω_r defined by $\Omega_0/(\Omega_0 + 2\Omega_1)$ roughly equals to 0.55 ($\pm$0.1) for both $|3D\rangle$ and $|3F\rangle$. It means that the $3D$ and the $3F$ line have the same polarization. Then, assuming that it also applies to neonlike barium, we obtained the collision strength ratio directly from the observed intensity ratio.

The observed intensity ratio is plotted in Fig. 5 together with the theoretical collision strength ratio obtained from relativistic distorted wave calculations by Zhang and Sampson.[6)] Since the theoretical collision strengths for $|3D\rangle$ and $|3F\rangle$ were obtained for the same scattered electron energy, the impact energy is slightly different for the two levels. The theoretical collision strength ratios are then plotted at the averaged impact energy in Fig. 5. The experimental intensity ratio was obtained by fitting Voigt line shapes to the data. The error bar in the figure represents the statistical error. Figure 4(b) shows the expanded spectrum for the region near the $3D$ and the $3F$ line together with the fitted line shapes. Although the peak around 4929 eV have not been identified, it was taken into account in the fitting procedure. To estimate the systematic error arising from possible superimposition of peaks, other two ways of fitting were performed: (i) without taking the unidentified peak into account; (ii) with assuming that there is another small peak around 4943 eV in addition to the unidentified peak around 4929 eV. These fitting procedures changed the ratio by about $\pm$10%, which is less than a half of the present statistical error.

As seen in Fig. 5, the present experimental intensity ratio is much larger than the theoretical collision strength ratio. In the theoretical calculation, only DE is taken into account. Although the indirect excitation processes, RC, II and RR, are evidently excluded in the present measurement, possibility of RE is not. Thus the disagreement between the experiment and the calculation is probably explained by taking the contribution of RE into account. Otherwise, the assumption on the magnetic sublevel distribution is wrong. However, large difference in the polarization between $3D$ and $3F$ is needed to consistently explain the difference between the experiment and the calculation. This conflicts with the theoretical results[23)] for neonlike iron and molybdenum.

In summary, we observed X-ray transitions in neonlike barium to obtain collision strengths for electron-impact excitation. The measurement was done at the electron energy which is just above the threshold to exclude indirect excitation. The present study showed utility of an experimental technique to measure relative collision strengths for electron-impact excitation of highly charged ions with excluding indirect processes. The disagreement between the experimental intensity ratio and the theoretical collision strength ratio is probably explained by taking the contribution of resonant excitation into account.

Acknowledgments

We would like to thank Prof. S. Nakazaki and Prof. T. Kagawa for fruitful discussion, Prof. Y. Yamazaki, Dr. T. Kambara and Dr. Y. Kanai for lending us the solid state detectors used in the present study.

1) H. F. Beyer, H. J. Kluge and V. P. Shevelko: *X-ray Radiation of Highly Charged Ions* (Springer, Berlin, 1997) Vol. 2, p. 122.
2) N. Nakamura, D. Kato and S. Ohtani: Phys. Rev. A **61** (2000) 052510.
3) M. Loulergue and H. Nussbaumer: Astron. Astrophys. **45** (1975) 125.
4) T. Kagawa, Y. Honda and S. Kiyokawa: Phys. Rev. A **44** (1991) 7092.
5) E. P. Ivanova and I. P. Grant: J. Phys. B **31** (1998) 2871.
6) H. L. Zhang and D. H. Sampson: At. Data Nucl. Data Tables **43** (1989) 1.
7) R. E. Marrs, M. A. Levine, D. A. Knapp and J. R. Henderson: Phys. Rev. Lett. **60** (1988) 1715.
8) R. E. Marrs, S. R. Elliott and J. H. Scofield: Phys. Rev. A **56** (1997) 1338.
9) P. Beiersdorfer, A. L. Osterheld, M. H. Chen, J. R. Henderson, D. A. Knapp, M. A. Levine, R. E. Marrs, K. J. Reed, M. B. Schneider and D. A. Vogel: Phys. Rev. Lett. **65** (1990) 1995.
10) S. Chantrenne, P. Beiersdorfer, R. Cauble and M. B. Schneider: Phys. Rev. Lett. **69** (1992) 265.
11) R. E. Marrs, P. Beiersdorfer, C. Bennett, M. H. Chen, T. Cowan, D. Dietrich, J. R. Henderson, D. A. Knapp, A. Osterheld, M. B. Shneider and J. H. Scofield: *Proc. Int. Symp. on Electron Beam Ion Sources and Their Applications*, No. 188 *AIP Conference Proceedings*, ed. A. Hershcovitch (American Institute of Physics, New York, 1989) p. 445.
12) F. J. Currell, J. Asada, K. Ishii, A. Minoh, K. Motohashi, N. Nakamura, K. Nishizawa, S. Ohtani, K. Okazaki, M. Sakurai, H. Shiraishi, S. Tsurubuchi and H. Watanabe: J. Phys. Soc. Jpn. **65** (1996) 3186.
13) H. Watanabe, J. Asada, F. J. Currell, T. Fukami, T. Hirayama, K. Motohashi, N. Nakamura, E. Nojikawa, S. Ohtani, K. Okazaki, M. Sakurai, H. Shimizu, N. Tada and S. Tsurubuchi: J. Phys. Soc. Jpn. **66** (1997) 3795.
14) N. Nakamura, J. Asada, F. J. Currell, T. Fukami, T. Hirayama, D. Kato, K. Motohashi, E. Nojikawa, S. Ohtani, K. Okazaki, M. Sakurai, H. Shimizu, N. Tada, S. Tsurubuchi and H. Watanabe: Rev. Sci. Instrum. **69** (1998) 694.
15) T. Mizogawa, Y. Awaya, Y. Isozumi, R. Katano, S. Ito and N. Maeda: Nucl. Instrum. Methods A **312** (1992) 547.
16) B. M. Penetrante, J. N. Bardsley, M. A. Levine, D. A. Knapp and R. E. Marrs: Phys. Rev. A **43** (1991) 4873.
17) *Table of Isotopes 8th Edition*, ed. R. B. Firestone and V. S. Shirley (John Wiley & Sons, INC., New York, N.Y., 1996).
18) S. Bashkin and J. O. Stoner, Jr.: *Atomic energy-level and grotrian diagrams* (North-Holland Publishing Company, New York, N.Y., 1978) Vol. 2.
19) M. A. Levine, R. E. Marrs, J. N. Bardsley, P. Beiersdorfer, C. L. Bennett, M. H. Chen, T. Cowan, D. Dietrich, J. R. Henderson, D. A. Knapp, A. Osterheld, B. M. Penetrante, M. B. Schneider and J. H. Scofield: Nucl. Instrum. Methods B **43** (1989) 431.
20) D. R. DeWitt, D. Schneider, M. H. Chen, M. B. Schneider, D. Church, G. Weinberg and M. Sakurai: Phys. Rev. A **47** (1993) R1597.
21) J. R. Henderson, P. Beiersdorfer, C. L. Bennett, S. Chantrenne, D. A. Knapp, R. E. Marrs, M. B. Schneider, K. L. Wong, G. A. Doschek, J. F. Seely, C. M. Brown, R. E. LaVilla, J. Dubau and M. A. Levine: Phys. Rev. Lett. **65** (1990) 705.
22) B. L. Henke, E. M. Gullikson and J. C. Davis: At. Data Nucl. Data Tables **54** (1993) 181.
23) H. L. Zhang and D. H. Sampson: Phys. Rev. A **41** (1990) 198.